

## Methanol Permeation Properties of Sulfonated Polyimide Membranes

Ken-ichi Okamoto\*, Liming Yang †, Tatsuaki Honda, Yan Yin, Makoto Yoshino, Kazuhiro Tanaka, and Hidetoshi Kita

Faculty of Engineering, Yamaguchi University, 2-16-1 Tokiwadai, Ube, Yamaguchi 755-8611, Japan

Fax: 81-0836-85-9601, e-mail: okamoto@po.cc.yamaguchi-u.ac.jp

† Lanzhou Institute of Chemical Physics, CAS, Tianshui Road, No. 342, Lanzhou, Gansu, 730000, P. R. China

Methanol permeation properties of main-chain and side-chain types of sulfonated polyimides (SPIs) were investigated by means of pervaporation (PV) and liquid-liquid permeation of methanol-water mixtures, compared with those of Nafion. In PV, the specific permeation fluxes of water and methanol components were five times and ten times, respectively, smaller for SPI membranes than for Nafion 115. The PV selectivities of water to methanol were about 2 for SPI membranes, but close to unity for Nafion 115. SPI membranes had much smaller methanol permeabilities than Nafion 115, but their proton conductivities in water were slightly larger or comparable to those of Nafion 117. As a result, most of SPI membranes showed more than three times larger ratios of proton conductivity to methanol permeability than Nafion, suggesting potential for direct methanol fuel cell application.

Key words: Sulfonated polyimide, Methanol permeation, Proton conductivity, Water uptake, Polymer electrolyte fuel cell

### 1. INTRODUCTION

In recent years there has been intense research interest in the development of proton exchange membrane (PEM) fuel cells for transportation, distributed power, and portable power applications [1]. Perfluorosulfonic acid membranes such as Nafion have excellent chemical and mechanical stability, as well as high proton conductivity. However, they have some disadvantages that limit their industrial applications. These include high cost, low operation temperature, and high methanol permeability. This promotes research interests in developing alternative non-fluorinated materials with low cost and high performance. So far, many kinds of sulfonated aromatic hydrocarbon polymers have been developed for the application of fuel cells [1,2].

Sulfonated polyimides (SPIs) are one of the promising materials among the PEMs investigated [3-9]. We synthesized two types of novel SPIs from 1,4,5,8-naphthalene-tetracarboxylic dianhydride (NTDA) and sulfonated aromatic diamines, of which the chemical structures are shown in Fig. 1. One is the main-chain type where the sulfonic acid groups are directly attached to the polymer backbone [5-7]. The typical example is the SPI derived from NTDA and 4,4'-bis(4-amino-phenoxy)biphenyl-3,3'-disulfonic acid (BAPBDS). The other is the side-chain type where sulfonic acid groups are attached to the side chains [8,9]. The typical example is SPI derived from NTDA and 2,2'-bis(3-sulfo-propoxy)benzidine (2,2'-BSPB) [8]. These SPIs displayed good proton conductivities and excellent water stability.

The PEMs should be barriers for the fuel transport or permeation. For direct methanol fuel cell application, the PEM should have high proton conductivity but low methanol permeability, in order to keep the high efficiency. In this study, methanol permeation properties of these two types of SPIs were investigated in comparison with those of Nafion 115 and 117.

### 2. EXPERIMENTAL

The SPIs, of which the chemical structures are shown in

Fig. 1, were prepared as described previously [5-9]. The SPIs (in triethylammonium salt form) were dissolved in *m*-cresol, and the solutions (5 wt%) were cast onto glass plates at 110 °C for 10 h. The as-cast membranes were soaked in methanol at 60 °C for 1 h to remove the residue solvent, and then proton-exchanged by immersing the membranes into 0.5 N H<sub>2</sub>SO<sub>4</sub> solution at 80 °C for 1 h and at room temperature for 5 h. After being thoroughly washed with ultra pure water, the membranes were dried in vacuo at 150 °C for 10 h. The membrane thickness was in the range of 20 to 60 μm.

Water uptake (WU) was calculated from equation 1:

$$WU = (W_s - W_d) / W_d \times 100\% \quad (1)$$

where  $W_d$  and  $W_s$  are the weights of dry and corresponding water-swollen film sheets, respectively.

Proton conductivity ( $\sigma$ ) was measured in water by an ac electrochemical impedance method over the frequency range from 100 Hz to 100 KHz (Hioki 3552) and  $\sigma$  was calculated from equation 2:

$$\sigma = L / (t_w w_w R) \quad (2)$$

where  $L$  is the distance between the two electrodes,  $t_w$  and  $w_w$  are the thickness and width of the membrane swollen in water, respectively, and  $R$  is the resistance value measured [7].

Pervaporation (PV) experiments were carried out by an ordinary method. The effective membrane area was about 20 cm<sup>2</sup> and the volume of feed solution was about 100 ml. The pressure of downstream side was maintained below 0.2 torr. The permeate was collected by a cold trap in liquid nitrogen. Feed and permeate composition was analyzed by gas chromatography. The separation factor of PV,  $\alpha_{PV}$ , was calculated from

$$\alpha_{PV} = y(1-x) / x(1-y) \quad (3)$$

where  $x$  and  $y$  are weight fractions of water in feed and permeate, respectively.

Methanol permeability of membranes was also measured using a liquid permeation cell composed of two compartments, which were separated by a vertical membrane. The membrane was first immersed in water for 2

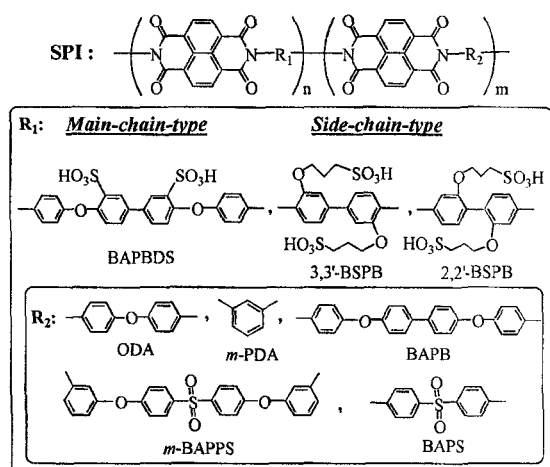


Fig. 1 Chemical structure of sulfonated polyimides.

h to get the water-swollen sample and then set into the measurement cell (effective area: 16 cm<sup>2</sup>). One compartment of the cell ( $V_A = 350$  ml) was filled with methanol feed solution, and the other compartment ( $V_B = 109$  ml) was filled with distilled water. The compartments were stirred continuously during the permeability measurement. The methanol concentration of the two compartments,  $C_A$  and  $C_B$ , were analyzed by gas chromatography. The methanol permeability,  $P_M$ , was calculated from equation 4:

$$q = A P_M \Delta C_{av} t / L$$

$$\Delta C_{av} = (C_{A0} + C_A - C_B) / 2 \quad (4)$$

where  $q$  is the methanol mol permeated into compartment B,  $t$  the measuring time,  $\Delta C_{av}$  the average methanol concentration difference between the two compartments during the permeation measurement, respectively.  $A$  and  $L$  are the area and thickness of the swollen membrane, respectively.  $C_{A0}$  is the initial methanol concentration in feed, and  $C_A$  and  $C_B$  are the methanol concentrations in feed and in permeate, respectively, at time  $t$ .

### 3. RESULTS AND DISCUSSION

#### 3.1 Membrane characterization

The SPIs prepared in this study are listed in Table I together with their IEC (calculated) and WU values. The side-chain type SPIs (NTDA-2,2'-BSPB, NTDA-3,3'-BSPB) with the same high IEC displayed very large WUs and strong anisotropic membrane swelling in water, namely, membrane swelling occurred only in membrane thickness direction but not in plane direction. Transmission electron microscopy (TEM) observation revealed that this type of SPI membranes have micro-phase separated structures composed of hydrophilic ionic domains and hydrophobic polyimide domains. Copolymerization with non-sulfonated diamines significantly reduced both WUs and membrane swelling, with keeping the anisotropy. The main-chain type SPI such as NTDA-BAPBDS, displayed a reasonably large WU, resulting from the high IEC. However, the membrane swelling was rather isotropic. The dimensional change in thickness was smaller than those of side-chain type SPIs, and the change in planar direction was much larger.

#### 3.2 Pervaporation

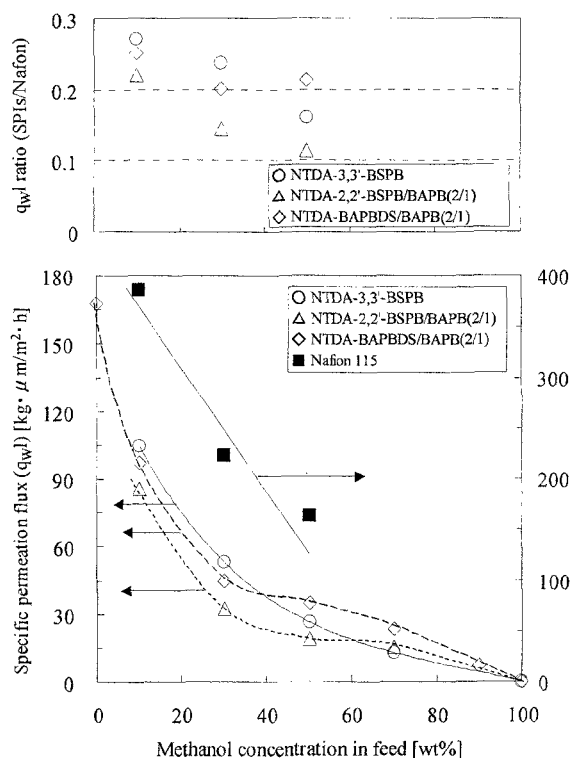
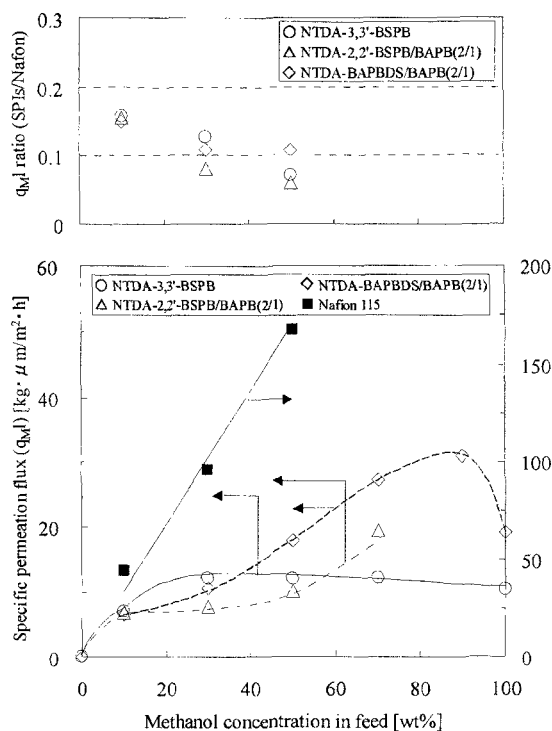
Fig. 2 (a) Feed composition dependence of specific permeation flux of water component  $q_{wl}$ .Fig. 2 (b) Feed composition dependence of specific permeation flux of methanol component  $q_{Ml}$ .

Fig. 2 shows feed composition dependence of (a) specific permeation flux of water component  $q_w$ , (b) specific permeation flux of methanol component  $q_M$ , and (c) separation factor  $\alpha_{PV}$  for water-methanol system in SPI membranes and Nafion 115 at 30 °C. As shown in Fig. 2 (a) and (b), in the case of Nafion 115, with an increase in methanol concentration in feed, the  $q_w$  decreased and the  $q_M$  increased, respectively. The change was rather large and displayed roughly linear relationship. In the range of methanol content above 50 wt%, the  $q_M$  increased significantly and the reproducible data were not available because of the significant membrane swelling. However, in the case of SPI membranes, quite different PV behavior was observed. With an increase in methanol content in feed, the  $q_w$  decreased initially significantly and then slowly, whereas the  $q_M$  increased initially relatively largely and then slowly. It is noted that the  $q_M$  was rather smaller for pure methanol than for methanol-rich solution. These results indicate that the SPI membranes were swollen more in water rather than in methanol. This is quite different from the case of Nafion being highly swelled in methanol.

The SPI membranes showed much smaller specific permeation fluxes than Nafion 115, that is, the  $q_w$  and  $q_M$  values were about ten times and five times, respectively, smaller for the former than the latter. As shown in Fig. 2 (c), the SPI membranes had  $\alpha_{PV}$  values of about two, indicating that they were somewhat more permeable to water than to methanol. On the other hand, Nafion 115 had  $\alpha_{PV}$  values close to unity, suggesting no PV separation through Nafion.

### 3.3 Methanol permeability

Methanol permeability ( $P_M$ ) of SPI membranes and Nafion 117 in highly water-swollen state was measured by means of liquid-liquid permeation experiments. The  $P_M$  values are summarized in Table I.

Nafion 117 showed a high  $P_M$  value of  $2.2 \times 10^{-6}$  cm<sup>2</sup>/s in 10 wt% methanol solution at 30 °C, which was in agreement with the literature values ( $2.3$  and  $2.6 \times 10^{-6}$  cm<sup>2</sup>/s) in 10

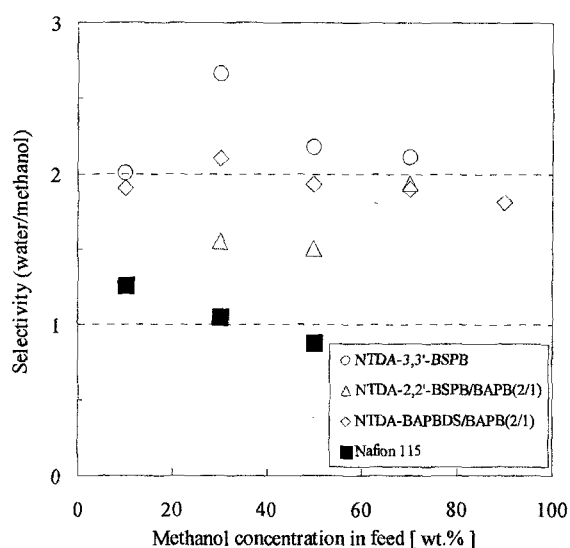


Fig. 2 (c) Feed composition dependence of separation factor  $\alpha_{PV}$  for water-methanol system.

wt% methanol at room temperature [10, 11]. With an increase in methanol content in feed up to 30 wt%, the  $P_M$  slightly increased up to  $2.7 \times 10^{-6}$  cm<sup>2</sup>/s. The similar slight increase in  $P_M$  was also reported for Nafion 117 [10]. The activation energy of  $P_M$  for Nafion 117 was about 16 KJ/mol, which was close to the value (18 KJ/mol) reported in literature [12].

The side-chain-type homo-SPIs, NTDA-2,2'-BSPB and NTDA-3,3'-BSPB, although having very large WUs, showed the smaller  $P_M$  values than Nafion 117, except for NTDA-3,3'-BSPB at 50 °C. The side-chain-type co-SPIs with much smaller WUs showed also much smaller  $P_M$  values compared with the corresponding homo-SPIs and Nafion. The main-chain-type SPIs also showed rather smaller  $P_M$  values than Nafion 117. The activation energies

Table I IEC, methanol permeability and proton conductivity of sulfonated polymer membranes

Membranes	IEC [meq/g]	WU <sup>a</sup> [wt%]	$P_M$ [10 <sup>-6</sup> cm <sup>2</sup> /s]			$\sigma$ [S/cm] <sup>d</sup>		$\phi = \sigma/P_M$ [10 <sup>4</sup> S·cm <sup>-3</sup> ·s]	
			30°C <sup>b</sup>	50°C <sup>b</sup>	30°C <sup>c</sup>	30°C	50°C	30°C	50°C
NTDA-2,2'-BSPB	2.89	220	1.05	2.06	1.15	0.14	0.22	13	10.7
NTDA-3,3'-BSPB	2.89	250	1.96	3.85	2.17	0.17	0.2	8.7	5.2
NTDA-2,2'-BSPB/BAPB (2/1)	2.02	44	0.34	0.51	0.66	0.055	0.07	16	14
NTDA-2,2'-BSPB/PDA (2/1)	2.32	55	0.74	1.21	1.05	0.11	0.125	15	10
NTDA-3,3'-BSPB/ODA (2/1)	2.23	73	1.21	1.62	1.36	0.13	0.14	11	8.6
NTDA-3,3'-BSPB/BAPS (2/1)	2.17	68	1.03	1.56	1.2	0.13	0.15	13	9.6
NTDA-3,3'-BSPB/BAPB (2/1)	2.02	62	0.69	1.33	0.92	0.082	0.11	12	8.3
NTDA-3,3'-BSPB/BAPPS (2/1)	1.95	—	0.45	0.95	0.91	0.076	0.097	17	10
NTDA-BAPBDS	2.63	75	1.14	2.58	—	0.16	0.19	14	7.4
NTDA-BAPBDS/BAPB(2/1)	1.89	—	0.86	1.19	1.05	0.13	0.15	15	13
SPS <sub>20</sub> <sup>c</sup>	1.41	—	0.52 <sup>f</sup>	1.19 <sup>g</sup>	—	0.05 <sup>f</sup>	0.086 <sup>g</sup>	9.6 <sup>f</sup>	7.2 <sup>g</sup>
Nafion 117	0.91	35	2.2	3.3	2.72	0.1	0.11	4.5	3.3

<sup>a</sup>Measured in water at 50 °C. <sup>b</sup>Methanol concentration in feed: 10 wt.%. <sup>c</sup>Methanol concentration in feed: 30 wt.%. <sup>d</sup>Measured in water. <sup>e</sup>Sulfonated poly(styrene) with sulfonation degree of 20 mol%. <sup>f</sup>Measured at 22°C. <sup>g</sup>Measured at 60°C.

of  $P_M$  for these SPIs were in the range of 17 to 27 KJ/mol, which are in consistent with those of other aromatic sulfonated polymers [12].

The difference in  $P_M$  between SPIs and Nafion 117 was much less than that in  $q_M$  for PV. This is due to the difference in the membrane swelling state. In the case of PV, the membrane was kept in dry state at the permeate side, whereas in the liquid-liquid permeation cell, both sides of the membrane were completely swelled, resulting in the less membrane swelling in PV than in liquid-liquid permeation.

### 3.4 Proton conductivity and ratio of proton conductivity to methanol permeability

The proton conductivity  $\sigma$  in liquid water and the ratio of  $\sigma$  to  $P_M$ ,  $\phi = \sigma/P_M$ , are also listed in Table I.

In the fully hydrated state (or in liquid water), the homo-SPIs with high IECs displayed larger proton conductivity (around 0.2 S/cm) than Nafion 117 (0.11 S/cm). The co-SPIs investigated here had fairly high IECs of more than 1.9 meq/g and showed high proton conductivities comparable to those of Nafion 117. It is considered that in the fully hydrated membrane with a fairly high IEC, the proton conduction paths are developed well enough to give a high proton conductivity, which also depends on IEC via carrier numbers. Nafion is known to have well-developed micro-phase separated structure and to have proton conducting channels connected from ionic domains, which give high proton conductivity in spite of low IEC of 0.91 meq/g. It is reasonable to consider that this channel structure causes the high permeation of methanol as well as of water. The BSPB-based homo-SPI membranes, although having micro-phase separated structure, don't seem to have such a clear channel structure, judging from the larger percolation threshold [8]. The present results are likely explained based on both the difference in morphology between Nafion and SPI membranes and the difference in the transport mechanism between proton conduction and methanol permeation.

The ratio  $\phi$  is an effective parameter evaluating the membrane performance in a DMFC system. As shown in Table I, most of the SPI membranes displayed larger  $\phi$  values than Nafion. Co-SPIs displayed slightly larger  $\phi$  values than the corresponding homo-SPIs. Although the proton conductivity of co-SPIs was smaller than the corresponding homo-SPIs, due to decreases in IEC as well as in water uptake, the reduction in methanol permeability was much more significant than the decrease in proton conductivity, resulting in comprehensive improvement of membrane performance.

To make a more clear understanding, Fig. 3 shows plots of normalized conductance vs. normalized methanol permeability for SPI membranes, using the  $\sigma$  and  $P_M$  values of Nafion as standards. It is clearly seen that most of the SPI membranes are better proton conductors and simultaneously better methanol barriers compared with Nafion membrane, suggesting potential for DMFC application.

## 4. CONCLUSION

The SPI membranes displayed much smaller swelling to methanol compared with Nafion, leading to much smaller methanol permeability. The ratio of the proton conductivity  $\sigma$  over the methanol permeability  $P_M$ ,  $\phi = \sigma/P_M$ , was more than three times larger for most of the SPIs than for

Nafion117. SPI membranes are better proton conductors and simultaneously better methanol barriers compared with Nafion membranes.

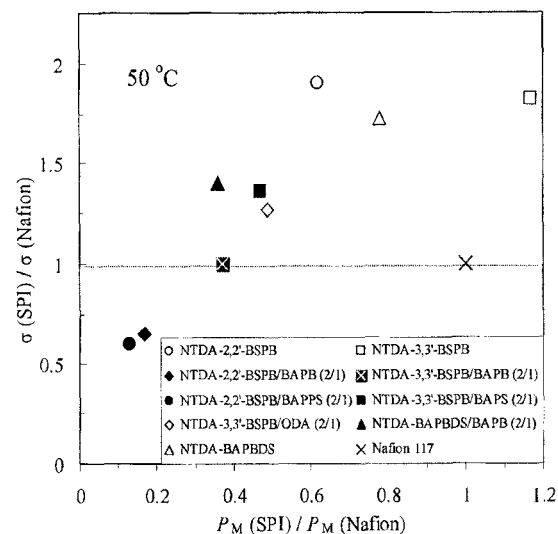


Fig. 3 Relative conductance and methanol permeability for SPI membranes compared with Nafion 117.

## ACKNOWLEDGEMENT

This work was supported partly by a Grant-in-aid for Exploratory Research (No. 14655294) from the Ministry of Education, Culture, Sports, Science, and Technology of Japan.

## REFERENCES

- [1] O. Savadogo, *J. New Mater. Electrochem. Systems*, **1**, 47 (1998).
- [2] M. Rikukawa and K. Sanui, *Prog. Polym. Sci.*, **25**, 1463 (2000).
- [3] S. Faure, R. Mercier, P. Aldebert, M. Pineri, and B. Sillion, *French Patent 9605707* (1996).
- [4] C. Genies, R. Mercier, B. Sillion, N. Cornet, G. Gebel, and M. Pineri, *Polymer*, **42**, 359 (2001).
- [5] J. Fang, X. Guo, S. Harada, T. Watari, K. Tanaka, H. Kita, and K. Okamoto, *Macromolecules*, **35**, 6707 and 9022 (2002).
- [6] X. Guo, J. Fang, O. Yamada, K. Tanaka, H. Kita, and K. Okamoto, *J. Polym. Sci., Polym. Phys. Ed.*, in press.
- [7] T. Watari, J. Fang, X. Guo, K. Tanaka, H. Kita, K. Okamoto and K. Hirano, *Kagakukougaku Ronbunshu*, **29**, 165 (2003). T. Watari, J. Fang, K. Tanaka, H. Kita, K. Okamoto and K. Hirano, *J. Membr. Sci.*, **230**, 111 (2004).
- [8] Y. Yin, J. Fang, H. Kita and K. Okamoto, *Chem. Letters*, **32**, 328 (2003). Y. Yin, J. Fang, T. Watari, K. Tanaka, H. Kita and K. Okamoto, *J. Mater. Chem.*, in press.
- [9] Y. Yin, J. Fang, Y. Cui, K. Tanaka, H. Kita and K. Okamoto, *Polymer*, **44**, 4509 (2003).
- [10] B. S. Pivovar, Y. Wang and E. L. Cussler, *J. Membr. Sci.*, **154**, 155 (1999).
- [11] J. Kim, B. Kim and B. Jung, *J. Membr. Sci.*, **207**, 129 (2002).
- [12] N. Carretta, V. Tricoli and F. Picchioni, *J. Membr. Sci.*, **166**, 189 (2000).